Program Digest, 2019 IEEE International Ultrasonics Symposium (IUS)
Glasgow, Scotland, October 6-9, 2019

Highly sensitive PZT transducer with integrated miniature amplifier for photoacoustic imaging

Chen Yang[1,2], Xiaohua Jian[2], Xinle Zhu[2], Jiabing Lv[2], Zhile Han[2], George Sergiadis[2,3,4], Yaoyao Cui[2]

[1]University of Science and Technology of China, Hefei, China
[2]Suzhou Institute of Biomedical Engineering and Technology, Chinese Academy of Sciences, Suzhou, China
[3]School of Electrical and Computer Engineering, Aritotle University, Thessaloniki, Greece
[4]Institute of Biological and Medical Imaging, Helmholtz Zentrum München, Neuherberg, Germany

Corresponding Email: cuiyy@sibet.ac.cn

***Abstract*—The design, fabrication and experimental characterization of a 20MHz lead zirconium titanate (PZT) transducer with integrated monolithic amplifier die for highly sensitive photoacoustic imaging is presented. The miniature amplifier is designed as a rectangular die for close connection to the transducer to match the output impedance to the connecting coaxial cable and provide front-end signal amplification. The measured frequency response of the integrated amplifier shows a wide bandwidth beyond 200 MHz, which is sufficient for wide band detection of photoacoustic signals. Both acoustical measurements and imaging experiments demonstrate that the fabricated prototype is capable of improving the signal-to-noise ratio (SNR) by over 10 dB.**

Keywords—photoacoustic imaging, detection sensitivity, PZT transducer, integrated miniature amplifier

I. Introduction

Photoacoustic imaging (PAI) is a rapidly evolving biomedical imaging modality that combines the superiority of high contrast and deep imaging depth by illuminating the tissue with short laser pulse and detecting signal acoustically [1, 2]. According to the configuration of the light and the acoustic detector, the implementations of PAI in biomedical applications can be categorized in to three forms [3]: photoacoustic tomography (PAT), photoacoustic microscopy (PAM) and photoacoustic endoscopy (PAE). The imaging depth and spatial resolutions are highly scalable based on different configurations. However, high detection sensitivity has always been a common pursuit in PAI.

Although the widely used acoustic transducers like lead zirconium titanate (PZT) transducer and capacitive micromachined ultrasonic transducer (CMUT) in ultrasound imaging are also adopted in PAI, the detected signal-to-noise ratio (SNR) of photoacoustic signal is much lower than that of ultrasound signal. When deep tissue rather than epidermis is imaged, light scattering and acoustic attenuation will cause strong attenuation to photoacoustic signals, resulting in limited imaging depth and deteriorated signal-to-noise ratio (SNR) [4]. Thus, high sensitivity acoustic detector is of particular importance in PAI. The most commonly used detectors in PAI are PZT transducer because of its well established fabrication technology and scalable sensitivity [5]. However, the impedance mismatch between the PZT element and the connecting coaxial cable usually leads to signal loss of several to tens dB, especially when thin and long cables are used [6]. Thus, a buffer amplifier is required to match the output impedance to the coaxial cable and amplify the signal in front-end.

In this work, we investigate the capability of a single element PZT transducer with integrated miniature amplifier for highly sensitive photoacoustic imaging. Section II describes the design of the proposed technique and the fabrication of the prototype transducer, as well as the experimental setup. Section III presents the results of the characterization and the imaging experiments. Section IV gives a conclusion and outlines the future work.

II. Methods

A. Assembly of the Transducer

Fig. 1(a) illustrates the assembly and integration scheme of the PZT transducer with integrated miniature amplifier. A homemade PZT transducer is designed as a rectangular element (3×1.5 mm). A thin graphite film was attached on the front surface of the PZT element as the matching layer. The backing layer was made of conductive silver paste (E-solder 3022, Von Roll Isola Inc.). The miniature amplifier is a rectangular die with a compact structure (820×760 μm) such that it could be integrated closely to the PZT element. For electrical connection between the PZT element and the amplifier die, power supply and signal output, a 0.3 mm thick flexible printed circuits board (fPCB) was fabricated. The amplifier die was attached on a well grounded gold plate using conductive epoxy (H20E, EpoTek) and wire bonded to the fPCB. The cross-section of the PZT transducer with integrated amplifier die is illustrated in Fig. 1(b). Two 1-meter-long coaxial cables were soldered on the corresponding pads on the fPCB for power supply and signal output. Then, the whole board was inserted into a customized housing for protection and isolation. At last, a 14-μm parylene film (Parylene-C) was

This work is funded by National Key Research and Development Program (2018YFC0116201, 2017YFC0110400 and Y716022601)), National Natural Science Foundation of China (11704397), Jiangsu Provincial Key Research and Development Plan (BE2017601).

coated on the transducer for acoustic impedance matching and electrical isolation from water. The fabricated prototype along with the fPCB is shown in Fig.1 (c). It should be noted that the current prototype has a relative large size mainly because of the size of the PZT transducer and the application scenario. Thanks to the compact structure of the amplifier, the size of the transducer can be further reduced to fit in various applications even in endoscopy.

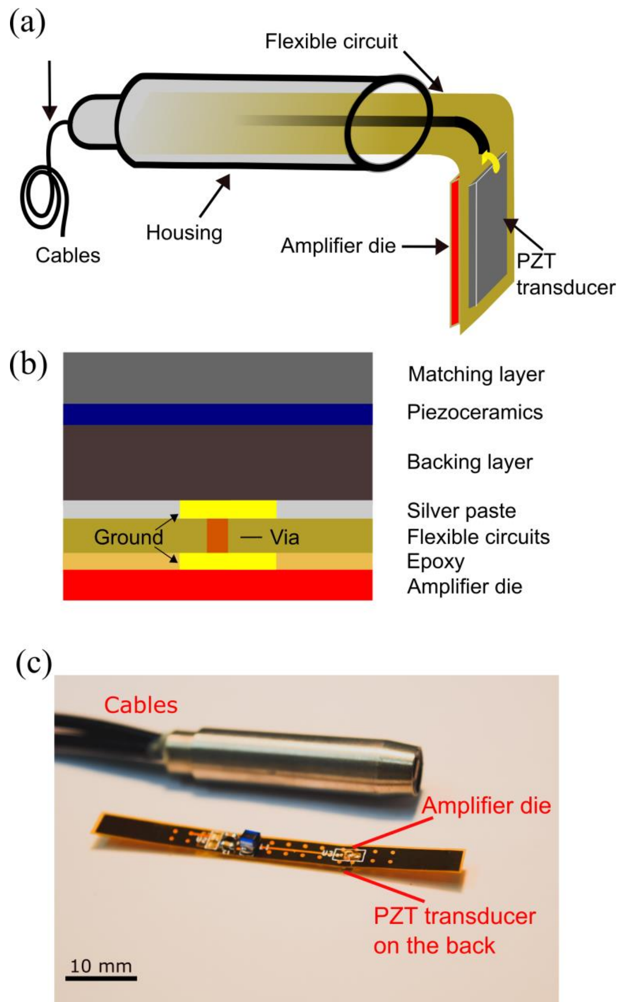

Fig. 1. (a) Schematic of the assembly of the transducer. (b) Cross-section of the PZT transducer with integrated amplifier die. (c) Photo of the fabricated prototype.

B. Electrical and Acoustical Measurements

To characterize the electrical performance of the fabricated PZT transducer, the impedance spectrum of the transducer is measured using an impedance analyzer (E991A, Keysight Technologies). To measure the frequency response of the amplifier die, a test board was designed and fabricated. A power supply was used to provide DC bias of the amplifier die. The signal source was coupled to the input of the amplifier die using an capacitor which has an equivalent impedance to the fabricated PZT transducer. The output frequency response was then measured using a network analyzer (E5061B, Keysight Technologies). The input power was set to -45 dBm.

To measure the detection sensitivity of the fabricated prototype, an acoustic measurement was set up in a water tank. A transmitter was driven by a 10-cycle and 5-Vpp sinusoidal burst to generate acoustic waves. The frequency of the burst was swept from 10 to 25 MHz with a step of 1 MHz. The prototype was fixed on a 3D motorized stage and placed straight forward to detect the acoustic waves. For comparison, a homemade PZT transducer without integrated amplifier (non-amplified transducer) was also used to receive signal at the same position. After the measurement, the transducer was replaced by a calibrated needle hydrophone (Precision Acoustics) to measure the actual acoustic pressure. The sensitivity was defined as the ratio of the amplitude of the measure output signal to the calibrated acoustic pressure. To further characterize the receiving performance, the transmitter was driven by a short ultrasonic pulse (5 ns, 150 Vpp). Both the prototype and the non-amplified transducer were used to detect the acoustic signal at different positions. The signal-to-noise ratio (SNR), defined as the ratio of the peak amplitude of the signal to the rms value of the noise, was calculated for both transducers.

C. Imaging Experiments

To characterize the imaging performance of the fabricated prototype, a backward-mode photoacoustic imaging system was developed, as shown in Fig. 2. The transducer is placed straight toward the sample, while the light illuminates the sample with an angle of 45 degree. The whole imaging head was fixed on a motorized stage for scan of the imaging area. The received photoacoustic signals were amplified by a low noise amplifier, averaged 8 times and bandpass filtered using MATLAB before image reconstruction. Each B-scan image was acquired by stacking a set of A-lines along the scan direction. A wire phantom constructed of two crossing tungsten wires was imaged. The wires are of 30 µm and 50 µm, respectively.

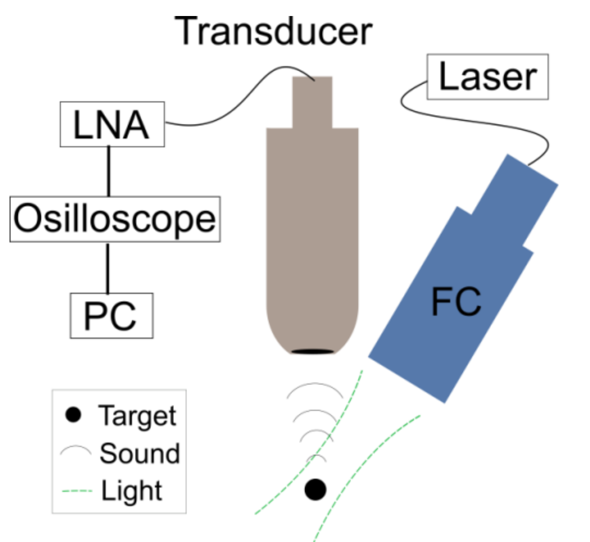

Fig. 2. Schematic of the setup of the imaging experiments. LNA: Low noise amplifier. UST: Ultrasound transducer. FC: Fiber collimator.

III. Results and Discussion

A. Characterization

Fig. 3(a) presents the measured electrical impedance spectrum of the fabricated PZT transducer. The center frequency is estimated to be ~18 MHz. The impedance at the center frequency is about 20 Ω. When connected directly to the coaxial cable with a characteristic impedance of 50 Ω, the impedance mismatch will lead to signal reflection and mismatch loss. Thus, a buffer amplifier is required. We propose in this work a compact integration between the PZT element and the amplifier. As shown in Fig. 3(b), the amplifier has a bandwidth beyond 200 MHz, which is sufficient for receiving of the wideband photoacoustic signals. It shows a flat response with over 25 dB gain from 10 to 50 MHz, which can completely cover the bandwidth of the fabricated PZT transducer.

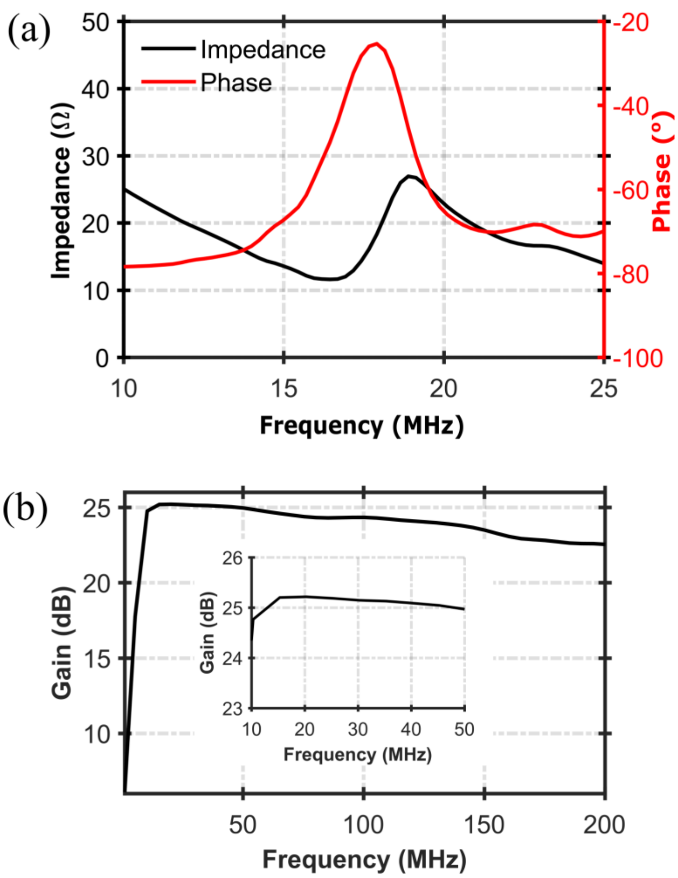

Fig. 3. (a) Electrical impedance spectrum of the PZT transducer. (b) Output frequency response of the amplifier. Inset: output frequency response from 10 to 50 MHz.

Fig. 4 presents the results of the acoustical measurements. The center frequency is measured to be 20MHz in water, which is slightly different from the results measured using impedance analyzer due to the effects of the attached cables and the acoustic loading. A significant enhancement of detection sensitivity can be found in Fig. 4(a). The sensitivity of the non-amplified transducer is 4.3μV/Pa at 20MHz, while that of the fabricated prototype is improved by ~15 times to 62.1μV/Pa. Besides, the SNR of the signal detected by the prototype is 10 dB higher than that detected by the non-amplified transducer, as shown in Fig. 4(b). Both transducers show decreasing SNR along the beam axis because of the diverging of the acoustic beam.

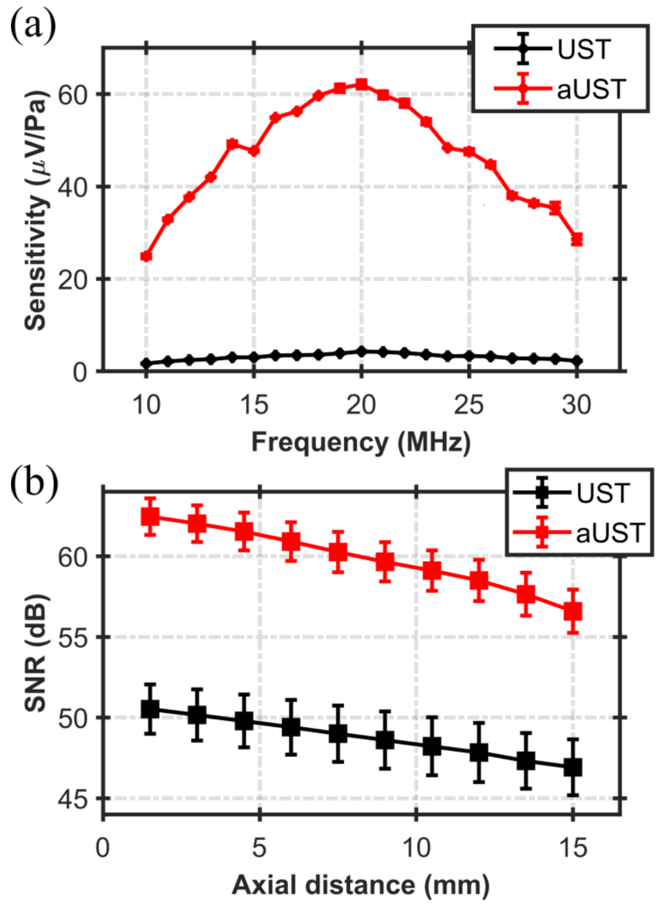

Fig. 4. (a) Measured sensitivity from 10 to 30 MHz. (b) Measured SNRs along the beam axis. UST represents the referenced non-amplified transducer. aUST represents the amplified transducer. The results are acquired from 3 individual tests and displayed as means ± SD.

B. Imaging Results

To characterize the imaging performance of the fabricated prototype, the wire phantom was imaged. For comparison, the experiment was also conducted using the non-amplified transducer. The configuration of the sound, light and phantom is illustrated in Fig. 5(a). The imaging head, composed of the transducer and the fiber collimator, is mechanically moved along the x axis to scan the targeted wires.

In Fig. 5(b), only the 50-μm wire can be observed, while the reconstructed image of the 30-μm wire is immersed in the background noise because of less optical absorption. In comparison, both targeted wires are clearly shown in Fig. 5(c) with improved contrast, implying that the prototype is able to improve the detection sensitivity and the imaging depth range. It should be noted that the crossing point of two wires is not well discriminated because the limited axial resolution is insufficient to resolve two wires when they get closing.

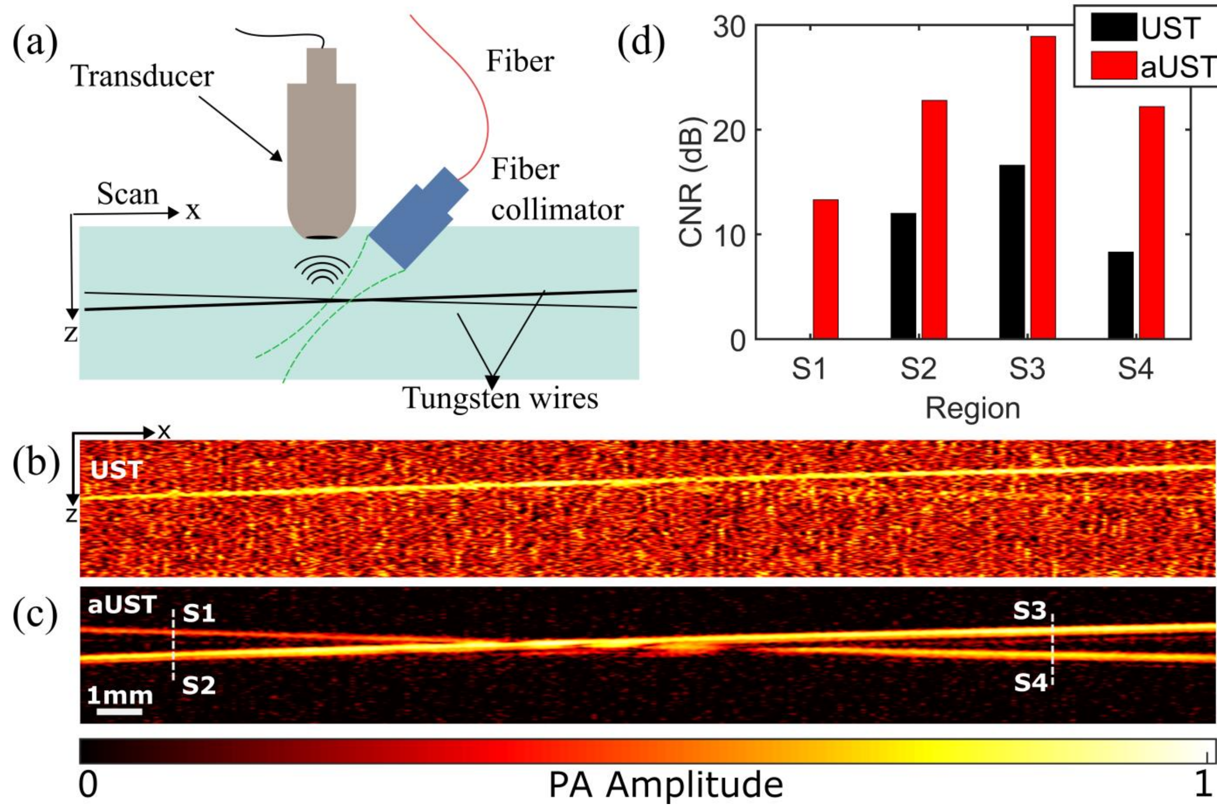

Fig. 5. (a) Configuration of the imaging experiment. (b) Photoacoustic image acquired using UST. (c) Photoacoustic image acquired using aUST. (d) Contrast-to-noise ratio (CNR) calculated at four spots labeled on (c). The CNR of UST at S1 is missing because the wire cannot be visualized. UST represents the referenced non-amplified transducer. aUST represents the amplified transducer.

The contrast-to-noise ratio (CNR), which is defined as the ratio of the mean amplitude of 10 pixels selected on the reconstructed wires to the rms value of the background noise, is calculated at four spots labeled by S1, S2, S3 and S4 on Fig. 5(c). For comparison, the CNRs of the corresponding spots on Fig. 5(b) are also computed. As shown in Fig. 5(d), there is a significant improvement of CNR by over 10 dB using the prototype, which agrees well with the results in the acoustical measurement.

IV. CONCLUSIONS AND FUTURE WORK

A prototype PZT transducer with integrated miniature amplifier for front-end signal amplification and output impedance matching has been designed, fabricated and characterized for highly sensitive photoacoustic imaging. This amplifier features a monolithic die and a wide bandwidth such that it can accommodate transducers of a wide range of sizes and frequencies.

The electrical performance of the PZT transducer implies that the direct connection between the transducer and the coaxial cable will lead to loss of sensitivity. Thus, a buffer amplifier is needed. The acoustical performance of the fabricated prototype demonstrates that our proposed method could improve the detection sensitivity by 10 dB.

The imaging experiments of wire phantom demonstrate the capability of highly sensitive photoacoustic imaging of the prototype. Compared with the non-amplified transducer, the prototype improves the CNR by 10 dB and enables visualization of larger depth range.

In our future work, ex vivo and in vivo experiments on animals will be performed to further confirm the imaging performance and demonstrate the potential biomedical applications of the prototype. Besides, higher frequency and larger bandwidth focusing transducers will be developed to achieve finer spatial resolutions.

REFERENCE

[1] P. Beard, "Biomedical photoacoustic imaging," *Interface Focus,* vol. 1, pp. 602-631, Aug 6 2011.

[2] S. Zackrisson, S. M. W. Y. van de Ven, and S. S. Gambhir, "Light In and Sound Out: Emerging Translational Strategies for Photoacoustic Imaging," *Cancer Research,* vol. 74, pp. 979-1004, Feb 15 2014.

[3] J. Meng and L. Song, "Biomedical photoacoustics in China," *Photoacoustics,* vol. 1, pp. 43-8, May 2013.

[4] V. Ntziachristos, "Going deeper than microscopy: the optical imaging frontier in biology," *Nature Methods,* vol. 7, pp. 603-614, Aug 2010.

[5] C. Lutzweiler and D. Razansky, "Optoacoustic Imaging and Tomography: Reconstruction Approaches and Outstanding Challenges in Image Performance and Quantification," *Sensors,* vol. 13, pp. 7345-7384, Jun 2013.

[6] C. Chen, S. B. Raghunathan, Z. L. Yu, M. Shabanimotlagh, Z. Chen, Z. Y. Chang*, et al.*, "A Prototype PZT Matrix Transducer With Low-Power Integrated Receive ASIC for 3-D Transesophageal Echocardiography," *Ieee Transactions on Ultrasonics Ferroelectrics And Frequency Control,* vol. 63, pp. 47-59, Jan 2016.